Working Paper Sustainability and Innovation
No. S 4/2012

David Dallinger
Gerda Schubert
Martin Wietschel

Integration of intermittent renewable power supply using grid-connected vehicles - a 2030 case study for California and Germany

Fraunhofer
ISI

Abstract

This paper describes a method to characterize the fluctuating electricity generation of renewable energy sources (RES) in a power system and compares the different parameters for California and Germany. Based on this method describing the fluctuation and residual load, the potential contribution of grid-connected vehicles to balancing generation from renewable energy sources is analyzed for a 2030 scenario using the agent-based simulation model PowerACE. The analysis reveals that integrating fluctuating RES is possible with less effort in California because of a higher correlation between RES generation and the load curve here. In addition, RES capacity factors are higher for California and therefore the ratio of installed capacity to peak load is lower. Germany, on the other hand, faces extreme residual load changes between periods with and without supply from RES. In both power system scenarios, grid-connected vehicles play an important role in reducing residual load fluctuation if smart charging is used. Uncontrolled charging or static time-of-use tariffs do not significantly improve the grid integration of RES.

Table of Contents

Page

1 Introduction 1

2 Characteristics of fluctuating generation 3

2.1 Method and input data 3

2.2 Evaluation criteria of energy fluctuation 4

2.2.1 Duration curve 5

2.2.2 Ramp rates 7

2.2.3 Interval availability 9

2.3 Evaluation of energy fluctuation 11

2.3.1 Total system load 11

2.3.2 Wind onshore 12

2.3.3 Solar power 14

3 Simulation method 16

4 Scenario definition 17

4.1 Electricity sector 17

4.2 Vehicle sector 18

5 Results 20

5.1 Residual load of the electricity system scenarios 20

5.1.1 Last trip charging 22

5.2 Time-of-use tariff 24

5.3 Balancing fluctuation with demand-side management 26

6 Conclusions 30

7 Appendix 33

8 Acknowledgements 35

9 References 35

1 Introduction

Renewable energy sources (RES) are essential to mitigate climate change and reduce the dependence on finite fossil energy sources [1]. However, both photovoltaic - the RES technology with the highest generation potential - and wind power - the RES technology with relatively low generation costs - face the challenge of fluctuating output [2]. Possible measures to reduce the impact of variable generation in a power system include:

- wider distribution via the transmission grids to include RES sources with different generation characteristics as well as additional demand centers;
- and/ or the installation of storage devices such as hydro pump storage, battery storage or compressed air storage;
- and/ or the response of demand by adapting consumption patterns (e.g. load shifting with industry processes or home appliances) and/ or by thermal storage (e.g. freezers, hotwater storage with heat pumps, etc.) which allow demand and supply to be decoupled.

Grid-connected electric vehicles (EVs) including pure battery electric vehicles (BEVs) and plug–in hybrid electric vehicles (PHEVs) can be used for demand response and as battery storage systems to feed power back into the grid (so-called vehicle-to-grid services) [3]. Compared to the other domestic appliances being discussed for load shifting, EVs enable long grid management times with low storage losses, but have significantly higher storage costs compared to the thermal storages used by smart grid devices such as freezers, air conditioning systems or heat pumps [4]. Because of battery degradation concerns and the high associated vehicle-to-grid costs, this paper focuses on EVs' load shifting abilities [5].

Demand response as tools to integrate variable renewable generation are discussed in [6]. This study concludes that real-time pricing (RTP) - the control approach also applied in this paper (see Chapter 3) – provides the flexibility needed to balance variable generation technically, but faces the obstacle of low stakeholder support. Currently, in the residential sector RTP is mainly used in research projects such as [7][8][9].

The impacts of EVs on the grid and their contribution to balancing fluctuating renewable generation have been discussed in various studies. The overall conclusion reached is that uncontrolled charging can result in a simultaneous surge

in demand with negative effects for the power system (e.g. an increase in the required peak capacity or grid overload) [10][11]. Delaying charging into night-time hours could help to overcome these issues, but will probably result in higher marginal emissions [12][13], which is contrary to the original principle of clean transportation. The possible contribution that EVs could make to integrate electricity from renewable energy sources (RES-E) which is discussed by [14], [15] and [16] therefore becomes a key research question. The parameters used to quantify the contribution of technologies to integrate RES-E are the reduction of ramp rates [17] as well the correlation between RES-E and electricity demand [18]. However, these parameters are not able to deliver a detailed quantification of a fluctuating time series. The fluctuating nature of renewable power influences the contribution EVs can make to balancing RES-E and therefore merits a high degree of attention. Chapter 2 supplements the conventional parameters with additional variablesin order to describe the framework conditions of fluctuating generation in a power system and the effects of EVs. Chapter 3 then gives a short description of the simulation approach used. A case study is made of Germany and California. Both areas are leaders in green technology adoption but have different climate conditions and load behavior. In Germany, the focus is on wind power, including offshore, and on photovoltaic with a very low capacity factor. The load peak here is in the winter. In California, solar power including photovoltaic and solar thermal is more important. In terms of wind energy, mainly onshore farms are being discussed, offshore installations are not included. The load peak is sharper and occurs during the summer months. A comparison of these two countries should deliver insights into the specific demand-side management capabilities of integrating RES-E into the grid. The main assumptions for a 2030 scenario for California and Germany are given in Chapter 4. Chapter 5 discusses the results using the quantification parameters defined and compares differences between California and Germany in the RES time series and RES integration. The final chapter 6 contains the conclusions.

2 Characteristics of fluctuating generation

2.1 Method and input data

Hourly resolved time series of RES-E representing the fluctuation in the investigated area are required as model input. Compared to the generation output of a single site, combining data from several sites results in a smoothing effect[1][19]. The energy output of the available data is scaled up to the assumed generation output in the scenario (see chapter 4). This method relies on simplified assumptions that weather, site-specific and RES technology data can be used to describe future RES-E output with a higher installed capacity. Methodological weaknesses result from limited weather data availability, technological change and changes in the geographic distribution of installation sites.

Table 2-1 gives an overview of the time series used as input for the simulation as well as the data source, underlying weather years, and information about the method of data preparation as well as the scenario in which the time series are used.

Table 2-1: Overview of the renewable energy input data

Time series	Scenario	Method of data preparation	Weather year	Source
Wind onshore GER	GER 2030	Measured	2008	[24]
Wind offshore GER		Weather data (measured)		[25][26][27]
Photovoltaic GER		Weather data (measured)		
Load GER		Measured		[24]
Wind CA	CA 2030	Weather data (measured and model data)	2005	[20] [21] [22] [23]
Solar Thermal CA				
Photovoltaics CA				
Load CA		Measured		

1 The smoothing effect describes a reduction in standard variation when more turbines and a higher separation of the turbines are used to generate one time series. The smoothing effect of a specified area is limited.

The time series for solar thermal, photovoltaics, load and wind output in California are taken from California's independent system operator (CAISO) [20]. The source distinguishes between different time series for photovoltaics (PV) and solar thermal (ST) (see Table 2.2). In this study, the time series are aggregated and weighted by the installed capacity to obtain single time series for PV and ST.

Table 2-2: Installed capacity in the "33 percent trajectory case" CAISO scenario

Technology	Installed capacity [MW]
Total photovoltaics (PV)	**6,661**
Large PV	3,527
Distribute PV	1,045
Customer Side PV	1,749
Out of State PV	340
Total solar thermal (ST)	**4,458**
Large Solar Thermal	4,058
Out of State ST	400
Wind	**9,436**

Source: [20]

The CA time series are generated using measured data from existing size as well as weather data from numerical weather prediction models. For details on CA time series see ([21], [22] and [23]).

The time series for wind onshore and load for the scenario GER 2030 are taken from [24] and represent real measured data from the year 2008 published by the German system operators. The PV and wind offshore time series are based on the wind speed and solar radiation measured in 2008 [25] [26]. The method describing the generation output is given in [27] and [28]. The weather year 2008 is used in the GER scenario because it represents an average wind generation year for Germany.

2.2 Evaluation criteria of energy fluctuation

To describe the generation of intermittent RES-E and the resulting residual load[2], the following three types of criteria are distinguished:

2 The residual load is defined as the total system load minus the fluctuating generation from RES. In this case, the residual load represents the generation needed from dispatchable power plants.

- Factors counting the available energy. These factors are the most common ones used but do not consider fluctuation and availability aspects. These factors are discussed and supplemented in chapter 2.2.1.
- The load change rate or the ramp rate. This factor describes the change in generation and load output between time steps. To compare different time series, the ramp rate factor as well as the mean and standard deviation of the ramp rate are considered in chapter 2.2.2.
- The interval availability is introduced to account for the average time intermittent power output is available (see chapter 2.2.3). This factor is related to the capacity credit but takes different power levels into account.

These evaluation criteria are used in chapter 5 to describe the contribution of PEVs to better integrate intermittent RES-E into the electricity grid. The simulation input data are also characterized using these criteria in order to specify the framework conditions.

2.2.1 Duration curve

Table 2-3: Nomenclature duration curve parameter

Parameter		Unit
cf_{pos}	Capacity factor	-
cf_{neg}	Capacity factor to characterize the negative residual load	
flh	Full load hours	h
T	Time period t Є T	8760 h/a
t	Time period of time step t Є T	h
E(t).	Energy produced in a certain time period	MWh
P_{rated}	Rated power	MW
$r_{cf0.8}$	Ratio between $cf_{Q<0.8}$ and $cf_{Q>=0.8}$	-
$cf_{Q<0.8}$	Capacity factor for sorted power values smaller than the 0.8 quantile	-
$cf_{Q>=0.8}$	Capacity factor for sorted power values equal to and bigger than the 0.8 quantile	-
Index		
t	Time step	-
Q	Quantile	-

The energy produced by generation units is often described using the capacity factor *cf* or the full load hours *flh*.

$$cf = \frac{\sum_t^T E(t)}{P_{rated} * T} \text{ and } flh = \frac{\sum_t^T E(t)}{P_{rated}} \qquad 2\text{-}1$$

respectively. Both factors are related to the energy produced *E(t)* in a certain time period T. P_{rated} is the rated power of a generation unit. In terms of the negative residual load, cf_{neg} and $cf_{y=0}$ are used to indicate the intercept with the y-axis. For fluctuating RES-E, part load (generation) operation dominates the duration curve (see Figure 2-1). Therefore, an additional factor, the capacity factor ratio $r_{cf0.8}$, is introduced to describe the energy production

$$r_{cf\,0.8} = \frac{cf_{Q<0.8}}{cf_{Q>=0.8}}. \qquad 2\text{-}2$$

$r_{cf0.8}$ is defined as the ratio between the capacity factor $cf_{Q<0.8}$ for sorted power values smaller than the 0.8 quantile and the capacity factor $cf_{Q>=0.8}$ for sorted power values equal to and bigger than the 0.8 quantile. The normalized area under the curve in Figure 2-1 represents the capacity factor and the areas left and right of the 0.8 quantile represent $cf_{Q>=0.8}$ and $cf_{Q<0.8}$ respectively. In addition, the maximal and minimal power P_{Max} and P_{Min}(1 hourly mean) and the correlation between fluctuating RES-E and the total system load are used as indicators for aggregated time series.

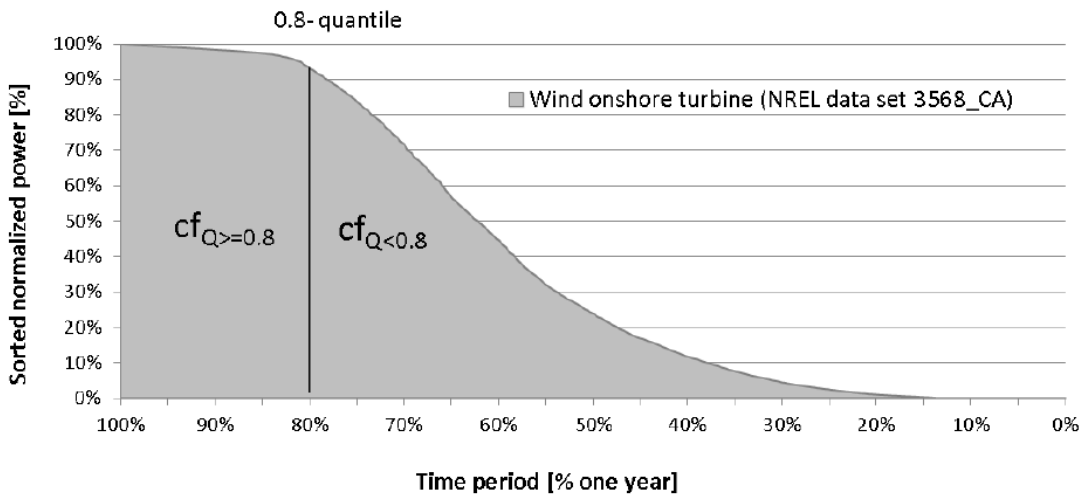

Figure 2-1: Duration curve of a wind turbine illustrating the characterization parameters used

Note: cf: capacity factor; Q: quantile; Source: Wind onshore turbine: [23], P_{max} = 100% = 10 MW

The information value of the capacity factor and the full load hours serve to compare the energy production of different technologies and installation sites. The capacity factor ratio allows for a more detailed analysis of the energy availability. A $r_{cf0.8}$ of 0.2 indicates that the energy generation in all 0.2-quantiles is the same. A $r_{cf0.8}$ of 1 shows that, for 20% of the time with the highest output, the energy production equals the output of the other 80% in the time period. A $cf_{Q>=0.8}$ close to 20% indicates a high share of full load operation (e.g. photovoltaics CA). Hence, lower values indicate higher part load operation (e.g. photovoltaics GER). A characterization of the generation data used follows in chapter 2.3.

2.2.2 Ramp rates

Table 2-4: Nomenclature ramp rate parameter

Parameter		Unit
P	Mean power of time step	MW
rr	Ramp rate	-
rrf	Ramp rate factor	-
P_{peak}	Peak power	MW
P_{rated}	Rated power	MW
T	Total time period	8760 h/a
t	Time period of time step t Є T	h
Index		
t	Time step	-

An important value to characterize the fluctuation of wind time series is the ramp rate [29][30][3]. The ramp rate *rr* is defined as:

$$rr(t) = \frac{P_{t+1} - P_t}{P_{rated} or P_{peak}} \qquad 2\text{-}3$$

where *P* is the mean power (hourly mean power) and n the counting index of one time step *t* in the time period T.[4] The values are normalized to the rated power P_{rated} for RES-E technologies and the peak power P_{peak} (1 hour mean)

3 The ramp rate is also described as power output increments

4 In this paper, a time resolution of one hour is used, T= 8760h.

for the system load. A positive ramp rate reflects an increase in either generation or load.

To quantify the ramp rate of different technologies and scenarios, the following parameters are introduced. The ramp rate factor *rrf* gives the area under the curve for positive rrf_{pos} and negative rrf_{neg} ramp rates (see Figure 2). The two areas are equal.[5] The ramp rate factor allows a comparison of the overall ramping of duration curves. Using the trapezoid function approach, *rrf* is calculated using Eq. 2-4:

$$rrf = \sum_t \frac{1}{T}(t_{t-1} - t_t)\cdot(rr_{t+1} + rr_t)\cdot 0.5 \quad ; rrf_{pos} \in rr > 0 \;\; ; \; rrf_{neg} \in rr < 0 \qquad (2\text{-}4)$$

In addition, the standard deviation $\sigma_{pos,neg}$, the mean value of *rr* $\mu_{pos,neg}$ and the intersection value of $x_{y=0}$ are used to characterize the fluctuation. Figure 2-2 illustrates the different parameters used to describe the ramping of fluctuation based on the German system load.

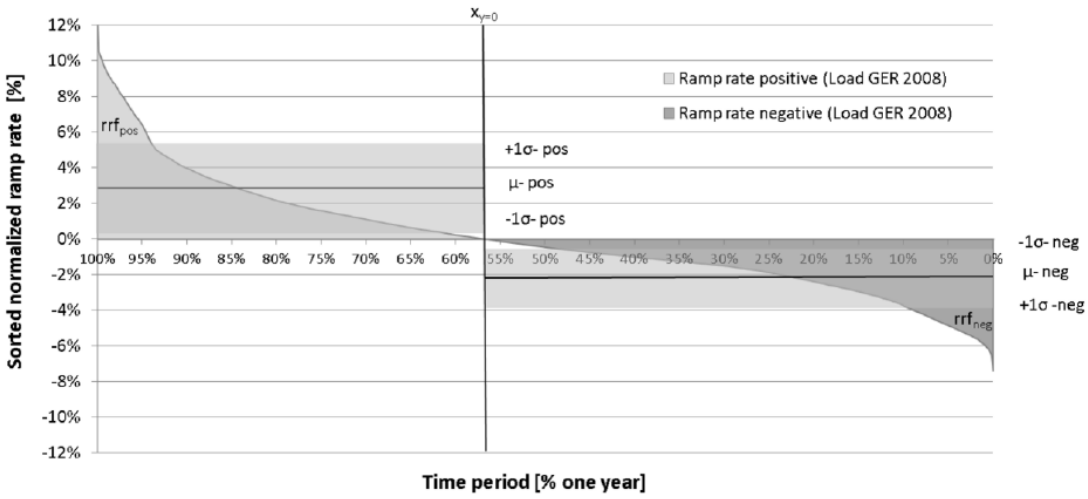

Figure 2-2: Sorted ramp rate for the German system load in 2008

Source: Load GER: [24] load year 2008, P_{max} = 100% = 77.950 GW

5 rrf_{pos} = rrf_{neg} is true if n is high or the first and the last state of power are the same. For n = 8760-1
rrf_{pos} = rrf_{neg} with high accuracy.

The ramp rate factor serves to compare the fluctuation of different technologies, installation sites and resulting load curves. The mean and standard deviation of the positive and negative ramp rates make it possible to characterize the irregularity of the fluctuation. An intersection with the y-axis higher than 50% indicates a more frequent negative ramp rate with less variation (see Figure 2-2) and the reverse is true for an intersection smaller than 50%. The generation and load data used are described in chapter 2.3.

2.2.3 Interval availability

Table 2-5: Nomenclature interval availability parameter

Parameter		Unit
$\Delta P_{normalized}$	Delta of normalized power in a time series	%
P_{min}	Minimum power	MW
P_{max}	Maximum power	MW
P_{peak}	Peak power of the load curve	MW
P_{rated}	Rated power of installed capacity	MW
X	Total number of events crossing section boundary	-
t	Time period of time step	h
Cor	Correlation	%
Index		
t	Time step	-
x	Number of events	-

The energy parameters and the ramp rates do not show for how long which fraction of fluctuating RES generation or residual load is available consecutively. To address this specific property, the average time availability t_0-t_4 of specific power levels section 0-4 is investigated. The power levels are defined as a section of the normalized delta power value $\Delta P_{normalized}$:

$$\Delta P_{normalized} = \frac{P(t)_{\max} - P(t)_{\min}}{P_{rated} or P_{peak}} \qquad 2\text{-}5$$

Note that $\Delta P_{normalized}$ depends on a specific time series. Hence, sections of photovoltaics and wind time series are different. The sections in detail are:

Section 0: 0% < P_t <=10%

Section 1: 10% < P_t <= 30%

Section 2: 30% < P_t <= 60%

Section 3: 60% < P_t <= 90%

Section 4: 90% < P_t <= 100%

The average availability of a section t_{Sec} is defined as the average time of all time periods t_n a section is available.

$$t_{Sec.} = \frac{\sum_x^X t_t}{X} \qquad 2\text{-}6$$

The total number of events x in which a time series crosses a section boundary is *X*. Figure 2-3 illustrates the values used to quantify the time availability.

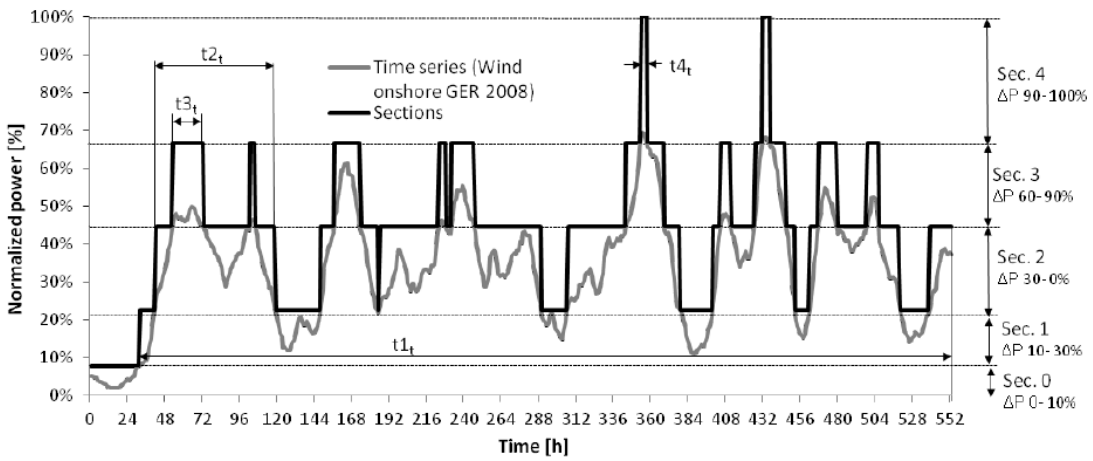

Figure 2-3: Average time availability for different sections of normalized power

Source: Time series (Wind onshore GER 2008): [24]

The average time availability is used to describe the reliability of a fluctuating energy source. The standard deviation of t is used for a more detailed assessment of average time availability. Related values in the literature are the capacity credit [31] and correlation (e.g. see [18]). Unlike the capacity credit, the average time availability also describes the mid and peak availability values. The correlation *Cor* is used to characterize the linear relation between the system load and supply from fluctuating generation.

2.3 Evaluation of energy fluctuation

In the following, all fluctuation time series used in the simulation are characterized using the parameters defined in chapter 2-2. All values are normalized to provide a basis for comparison.

2.3.1 Total system load

The total system load is the departure point for analyzing the effect of fluctuating RES-E. The load curve and its correlation with RES-E generation determine the residual load. Figure 2-4 shows the load duration curve for Germany (GER) and California (CA). The differences occur due to individual consumer and industry demands. Air conditioning is the most obvious load which is typical for California. This is the reason for the very steep CA curve within 10% of the highest values. The parameter $cf_{Q>=0.8}$ (14.3% compared to 18%) indicates that peak generation is needed for fewer hours in CA than in GER, where the value close to 20% shows that a high load occurs for numerous hours over the year. Also the values for the capacity factor *cf* and the minimum power P_{min} are characteristic for the specific conditions in CA.

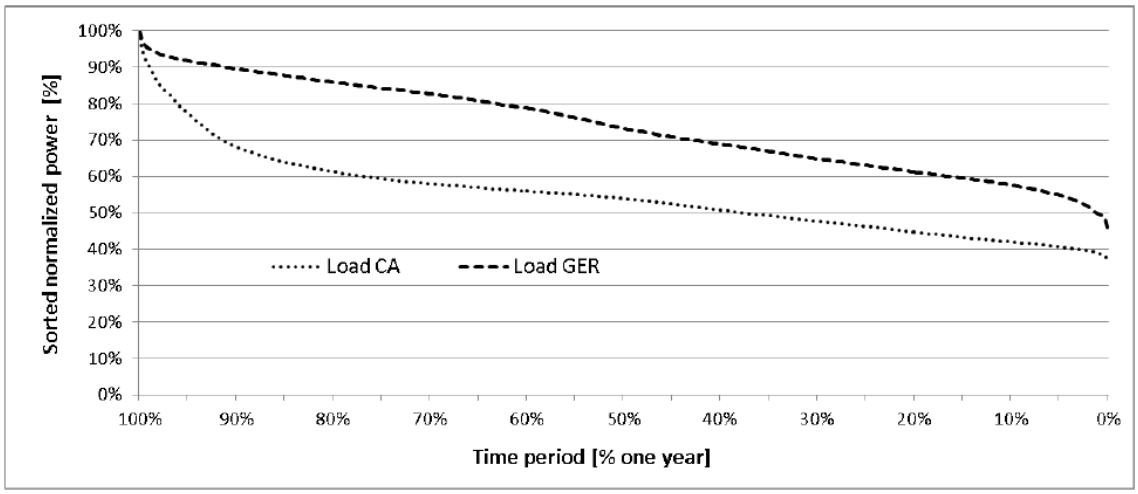

Figure 2-4: Sorted duration curves of the total system load for Germany and California

Source: GER: Germany [24] weather year 2008, P_{max} = 100% = 77.950 GW; CA: California [20], P_{max} = 100% = 63.545 GW

In terms of the ramp rates, GER shows a higher value (*rrf* 1.19% compared to 1.05%). Especially in the morning hours, a high ramping up is typical for Germany. In this context, X_y=56.40% indicates that ramping down occurs more often in GER and is not as rapid as ramping up ($\mu_{pos} > \mu_{neg}$). In CA, ramping up is also faster than ramping down, but not as fast as in GER. The discussed parameters are summarized in Table 2-6.

Table 2-6: Selected parameters used to characterize the load curve

Load GER 2008				Load CA 2005			
cf	73.53%	rrf_{pos}	1.19%	cf	54.58%	rrf_{pos}	1.05%
$cf_{Q>=0.8}$	17.99%	μ_{pos}	2.74%	$cf_{Q>=0.8}$	14.27%	μ_{pos}	2.12%
$r_{cf0.8}$	0.32	μ_{neg}	-2.12%	$r_{cf0.8}$	0.35	μ_{neg}	-2.07%
P_{min}	44.70%	$x_{y=0}$	56.40%	P_{min}	36.29%	$x_{y=0}$	50.59%

Source: Own calculation data basis [24], and [20]

2.3.2 Wind onshore

Onshore wind is the fluctuating energy source with the highest installed capacity in Germany[6] and worldwide. The available time series are very accurate and smoothing effects in areas with high installed capacity are well known (compare aggregated data with data of single turbines in Figure 2-5). Onshore wind time series for CA and GER indicate a similar peak mean power output P_{max} of around 80% (see P_{max} in Tab. 2-7) of total installed capacity. The CA values of $cf_{Q>=0.8}$ and $rcf_{0.8}$ are higher than for GER which demonstrate a higher availability of peak as well as off-peak generation hours.

6 The installed wind onshore capacity in Germany was about 30 GW at the end of 2011.

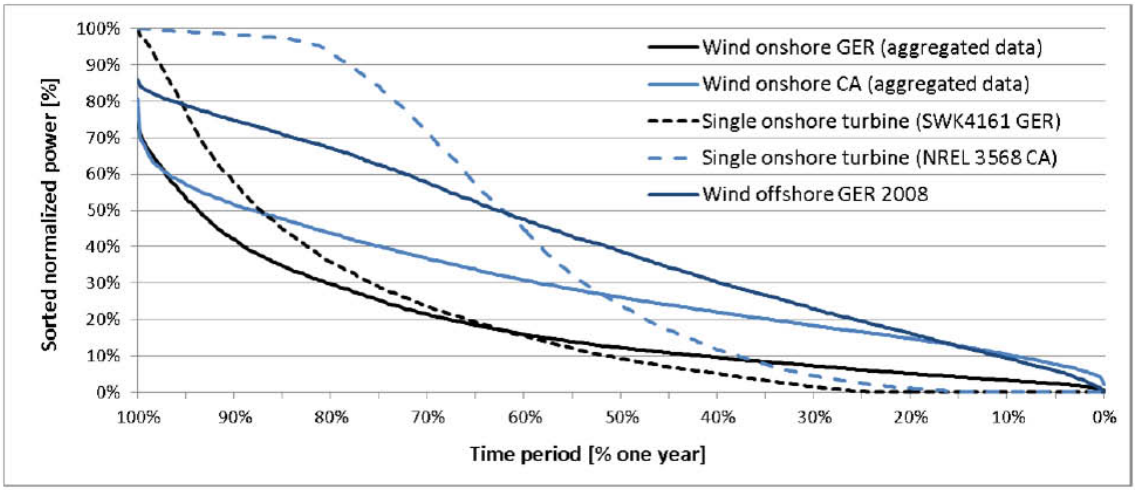

Figure 2-5: Sorted duration curves for wind

Source: SWK 4161 GER:[32]; NREL 3568:[23]; wind onshore CA: [20]; wind onshore GER: [25]

The CA time series also show a higher ramp rate factor *rrf* and mean ramp rates μ. Besides specific weather conditions, the method used to generate the CA time series could also be a reason for this result. The CA intersection with the x- axis $x_{y=0}$ is 47.14%. Consequently, ramping down is more rapid ($\mu_{neg} > \mu_{pos}$) in California. Ramping down and up in GER shows similar values with $x_{y=0}$ close to 50%.

German offshore wind generation is expected to produce more energy and nominal power than onshore wind. Offshore ramping is higher than onshore ramping. One possible reason is the limited number of available wind speed measurement points used to generate the time series as well as the expected concentration of installed capacity on an area with similar wind speed characteristics. To generate the time series, a multi-turbine power curve [33] with a maximal rated power output of 89% is used. The parameters are summarized in Table 2-7.

Table 2-7: Selected parameters to characterize the wind time series.

Wind onshore GER 2008				Wind offshore GER 2008				Wind onshore CA 2005			
cf	19.99%	rrf_{pos}	0.66%	cf	40.65%	rrf_{pos}	1.61%	cf	28.88%	rrf_{pos}	1.25%
$cf_{Q>=0.8}$	10.00%	μ_{pos}	1.34%	$cf_{Q>=0.8}$	15.00%	μ_{pos}	3.21%	$cf_{Q>=0.8}$	10.58%	μ_{pos}	2.21%
$r_{cf0.8}$	1.00	μ_{neg}	-1.30%	$r_{cf0.8}$	0.58	μ_{neg}	-3.19%	$r_{cf0.8}$	0.58	μ_{neg}	-2.63%
P_{min}	0.56%	$x_{y=0}$	49.72%	P_{min}	0.13%	$x_{y=0}$	49.86%	P_{min}	2.02%	$x_{y=0}$	47.14%
P_{max}	82.51%			P_{max}	85.93%			P_{max}	80.75%		

Source: Own calculation data basis [24], [25] and [20]

The interval availability of wind is heavily dependent on weather events. The standard deviation of the average interval availability time is very high, especially in section 1 (Quartile 10-30%). In CA, the interval availability is higher (section 1-3) except for the peak hours (section 4). Hence, weather events with a long and high output are more likely for GER. Periods with a long absence of significant capacity are also more often and longer in GER (section 0). Analyzing the availability for different hours of the day shows a peak output during the evening (17-24 hour clock) in CA, whereas no clear trend is apparent for GER. The parameters for wind availability are summarized in Table 2.8.

Table 2-8: Selected parameters to characterize the interval availability of wind onshore time series

Wind onshore GER 2008					Wind onshore CA 2005				
Quantile	**% of peak power**	**Number of events**	**t mean**	**t_σ**	**Quan-tile**	**% of peak power**	**Number of events**	**t mean**	**t_σ**
Sec. 0	< 8.8	173	16.5	20.5	Sec. 0	< 9.9	122	6.6	7.2
Sec. 1	8.8 - 25.1	173	34.1	61.0	Sec. 1	9.9 - 25.6	122	64.9	127.8
Sec. 2	25.1 - 49.7	100	24.8	29.3	Sec. 2	25.6 - 49.2	267	16.7	19.3
Sec. 3	49.7 - 74.3	47	15.9	14.0	Sec. 3	49.2 - 72.9	168	6.7	6.1
Sec. 4	>74.3	16	6.1	3.8	Sec. 4	>72.9	2	3.0	0.0

Source: Own calculation data basis [24]and [20]

2.3.3 Solar power

CA parameters for photovoltaics and solar thermal show very high energy output and availability of nominal power during the main hours of generation (indicated by a high $cf_{Q>=0.8}$). The energy output in Germany is less than half that generated in California ($cf_{CA\ PV}$= 24.7% compared to $cf_{GER\ PV}$= 10%). The peak of simultaneous generation is 64.5% of the nominal power in GER, whereas the CA time series show a much higher P_{max}. The absolute ramping is also higher in CA ($rrf_{GER,PV}$=1.35; $rrf_{CA,PV}$=3.18; $rrf_{CA,ST}$=3.2) as are the CA average ramp rates (Figure 2-6). One possible explanation for this is the higher share of direct radiation in CA, which leads to simultaneous generation and a greater tendency towards very large installations as well as PV tracing systems. In terms of the solar thermal generation time series, the higher ramp rates also indicate the use of thermal storage. The solar thermal power plants are operated to maximize electricity output during peak hours.

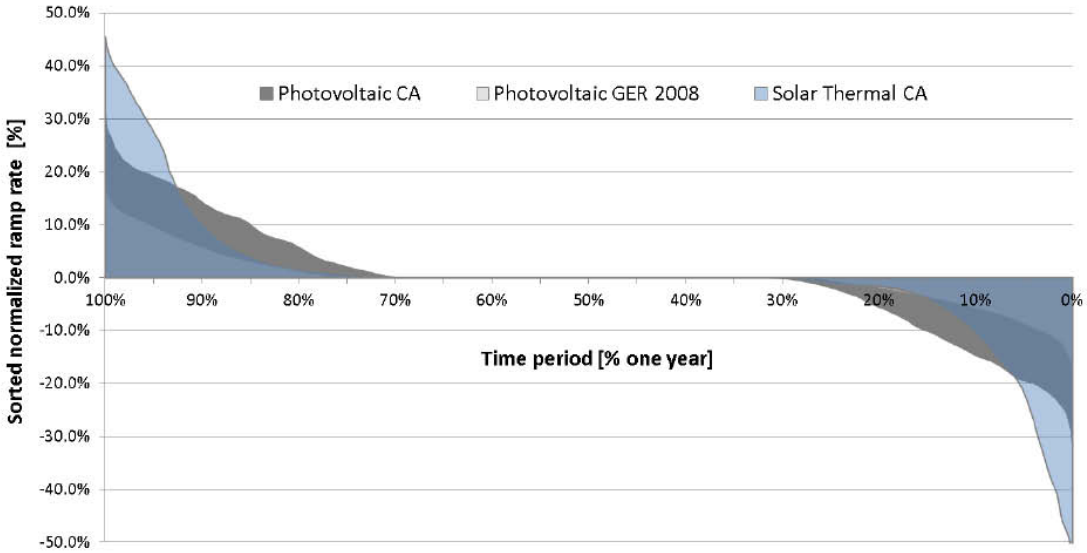

Figure 2-6: Sorted ramp rates for solar generation in California and Germany

Source: Photovoltaics GER 2008: Data set [26] method [28]; solar thermal and photovoltaics CA: [20]

For solar thermal generation, ramping down and ramping up are more evenly balanced than for photovoltaics. Photovoltaics shows a tendency to more rapid ramping down and to a greater extent for CA. The parameters used for solar availability are summarized in Table 2-9.

Table 2-9: Selected parameters to characterize the solar time series.

Photovoltaics GER 2008				Photovoltaics CA 2005				Solar Thermal CA 2005			
cf	10.02%	rrf_{pos}	1.35%	cf	24.66%	rrf_{pos}	3.18%	cf	25.81%	rrf_{pos}	3.20%
$cf_{Q>=0.8}$	7.57%	μ_{pos}	4.36%	$cf_{Q>=0.8}$	15.45%	μ_{pos}	7.60%	$cf_{Q>=0.8}$	16.88%	μ_{pos}	10.79%
$r_{cf0.8}$	3.10	μ_{neg}	-4.71%	$r_{cf0.8}$	1.68	μ_{neg}	-10.40%	$r_{cf0.8}$	1.89	μ_{neg}	-9.37%
P_{min}	0.00%	$x_{y1=0}$	72.76%	P_{min}	0.00%	$x_{y1=0}$	69.76%	P_{min}	0.00%	$x_{y1=0}$	70.36%
P_{max}	64.62%	$x_{y2=0}$	29.47%	P_{max}	98.42%	$x_{y2=0}$	30.61%	P_{max}	95.72%	$x_{y2=0}$	34.14%

Source: Own calculation data basis [25], [28] and [20]

3 Simulation method

The effects of PEVs on the electricity system are investigated by combining the following approaches: a stochastic model to determine mobility behavior, a distributed vehicle-based optimization model minimizing vehicle charging costs, and an agent-based electricity market equilibrium model to estimate variable electricity prices and power plant utilization.

Electricity prices for a scenario with a high share of RES generation are calculated using the agent-based simulation model PowerACE [34]. This model provides a detailed representation of the German electricity sector and simulates reserve markets and the spot market. Spot market prices are calculated on an hourly level for an entire year. The merit-order follows the variable electricity generation costs of power plants which are mainly comprised of fuel and CO_2 prices as well as start-up costs. For intermittent RES-E, the variable costs are assumed to be zero. Hence, prices are low in hours with high renewable power supply or a low residual load. This merit-order effect [35], [36],[37] of RES-E in a uniform price auction is used to send a price-based control signal to the PEVs.

Vehicles are modeled as agents receiving a control signal that consists of a price forecast of the electricity auction and an individual price component depending on the transformer utilization of a distributed grid [38]. A graph search optimization algorithm is used to find the charging spots with the lowest price [5]. The optimization time period is influenced by the mobility behavior, which is modeled individually for 12,000 agents using driving probabilities. In terms of charging strategies, two cases are distinguished. In the first case, PEVs start charging after the last trip of the day without optimizing charging times. In the second case, vehicles can charge while parked at home or at work and charging optimization is used. The optimization time period depends on the grid management time or the time between two trips minus the charging and driving time and is known when vehicles return from a trip. The simulation is done using quarter hourly time intervals for vehicles and mobility behavior. Price sensitivities and the plug-in behavior of consumers are not considered. It is assumed that the vehicles are plugged in within a quarter hour after returning from a trip. The optimization algorithm selects the time step with the lowest price even if the price differences to other time steps are not sufficient to provide significant incentives to consumers. The simulation does not consider concerns about battery aging such as accelerated aging due to a high state of charge over a longer time period, or concerns about battery temperature restricting charging.

4 Scenario definition

The scenarios include certain assumptions about the future. This is necessary because the framework conditions in terms of the market penetration of PEVs or the installed capacity of RES are not sufficient to answer our research question. In order to analyze the effect of fluctuating renewable energy generation from wind power and photovoltaic, as well as the contribution of PEVs towards balancing these RES-E, we had to construct a scenario for 2030. In the following scenario, assumptions for Germany are presented which distinguish between the electricity sector and the vehicles sector. In addition, a sub-scenario for California is used to take into account the different fluctuation of RES-E there.

4.1 Electricity sector

In order to investigate the contribution of PEVs to integrating RES-E into the grid, scenarios are defined based on surveys available in the literature. These scenarios are used to create an environment with very high RES penetration (necessary to reach the CO_2 reduction goal of the German government). The main scenario used “GER 2030” refers to the “Lead Scenario 2010”, which was part of a survey investigating high RES penetration in Germany made on behalf of the German Federal Ministry for the Environment, Nature Conservation and Nuclear Safety [39]. Other surveys of the German energy sector, [40] and [41], do not account for nuclear phase-out or the time period until 2030[7]. The “Lead Scenario 2010” was selected because this study is best suited to investigating the effects of fluctuating generation. However, in order to enable scenario-independent general findings and conclusions to be drawn, a detailed analysis is made of the input parameters so that the effects of the scenario estimations are transparent. A sub-scenario for California “CA 2030” is used based on data from a 2020 CAISO study [20] in order to consider the different load curve, RES technology composition and fluctuation characteristics in CA. The CA 2030 scenario is scaled to the same energy generation share of fluctuating RES-E as the GER 2030 scenario to enable better comparability (see Table 4-1).

7 To some extent these studies are influenced by stakeholders. The “Lead Scenario 2010” is supported by policymakers and companies interested in a high RES penetration and strong reduction of CO2 emissions.

Table 4-1: Intermittent generation and electricity demand for GER 2030 and CA 2030

Scenario		Wind on-shore	Wind off-shore	Photo-voltaic	Solar Thermal	Share of fluctuating RES-E (peak load; generation)	Total electricity demand (peak load; generation)	Unit
GER 2030*	Capacity	37.8	25	63	-	162%	77.8	GW
	Generation	87.038	95	56.993	13.3	47.60%	502.1**	TWh
CA 2030**	Capacity	28.2	-	19.9	13.3	96.70%	63.5	GW
	Generation	71.403	-	43.051	30.158	47.60%	303.806	TWh

Source: * Lead Scenario 2010 [39]; ** Energiereport IV [42];*** Proportion of technologies and fluctuation from [20]. The generation share of intermittent RES is scaled to 47.6% and the same value of the Lead Scenario, 2010 respectively

The hourly characteristics of RES generation and the load curve were already discussed in chapter 2. Imports and exports of electricity and storage technologies such as hydro pump storage are not taken into account.

To indicate the dispatchable supply side, the merit order of power plants is generated using primary energy and CO_2 prices from [39]. Based on the current German power plant mix, it is assumed that all power plants which reach the end of their useful life in 2030 will be replaced by gas turbine power stations and combined-cycle plants to guarantee high ramping capability.

4.2 Vehicle sector

The penetration scenario for PEVs follows [43], a study investigating a 100% penetration of alternative vehicles (HEVs, PHEVs, BEVs and FCV) for Japan in 2050. The penetration of PHEVs and BEVs was adapted to the German passenger vehicle market by specifying two EV concepts divided into PHEVs with 4.5 kWh or 12 kWh and BEVs with 15 kWh or 30 kWh usable battery storage (see Table 4-2). The assumptions with regard to the energy use of PEVs imply a reduction in weight as well as in air and rolling resistance compared to today's average vehicles [44-46][8]. The total penetration with PHEVs in 2030 is 12 million or 24% of the total passenger vehicle fleet, accounting for a PEV share of over 80%. This scenario is classified as optimistic (for further estimations, see

8 Values in the range of: weight 800-1400 kg, drag coefficient 0.2 – 0.26 and rolling resistance 0.0045 – 0.006.

[47][48][49]). For the CA 2030 scenario [50][9], the PEV's share of the total fleet equals the GER scenario and results in a total PEV penetration of 6.8 million[10].

Table 4-1: Passenger vehicle types

Device	Type*	Usable storage [kWh]	Grid connection power [kW]	Equivalent energy use [kWh_{el}/km] **	CA 2030 (6.7 million PEVs)	GER 2030 (12 million PEVs)
1	PHEV (25)	4.5	4	0.18	31.60%	31.60%
2	PHEV (57)	12	4	0.21	50.40%	50.40%
3	BEV (100)	15	8	0.15	13.90%	13.90%
4	BEV (167)	30	8	0.18	4.00%	4.00%

Comments: * In brackets hypothetical driving range in km; ** At grid connection including a charging efficiency of 94%.

The allocation of the different vehicle types is shown in Table 4-2. In total, 12 thousand PEVs are modeled for GER 2030, which represent 12 million PEVs. In other words, the operation of one vehicle is scaled-up by a factor of 1,000.

Table 4-3 summarizes the power and storage capacity of the resulting vehicle fleet for the two scenarios. A fleet of PEVs provides high power with a relatively low usable amount of battery storage. The power/energy ratio of the total fleet for CA 2030 and GER 2030 is 0.44. By comparison, German pumped storage plants provide 7.76 GW with a rated volume of 224.31 GWh (ratio: 0.035).

9 Total passenger vehicles 28,320,000.

10 This assumption is similar to [45] which supposes a penetration of 6.63 million PEVs.

Table 4-2: Resulting power and energy values of the vehicle fleet scenarios

	CA 2030			GER 2030		
Type	**Vehicles [thousand]**	**Connection power [GW]**	**Storage capacity [GWh]**	**Vehicles [thousand]**	**Connection power [GW]**	**Storage capacity [GWh]**
PHEV (25)	2,150	8.60	9.68	3,885	15.54	17.48
PHEV (57)	3,430	13.72	41.16	6,585	26.34	79.02
BEV (100)	945	7.56	14.18	1,230	9.84	18.45
BEV (167)	275	2.20	8.25	300	2.40	9.00
Sum	**6,800**	**32.08**	**73.26**	**12,000**	**54.12**	**123.95**

5 Results

5.1 Residual load of the electricity system scenarios

To evaluate how PEVs can help to integrate RES into the grid, the remaining residual load is used as a benchmark. The assessment uses the parameters defined in chapter 2. The most important parameters for the residual load[11] in the scenarios CA 2030 and GER 2030 are summarized in Table 5.1.

Table 5-1: Evaluation parameters, residual load (RS) for California (CA) versus Germany (GER)

RS GER 2008				RS CA			
cf_{pos}	39.1%	rrf_{pos}	2.00%	cf_{pos}	28.9%	rrf_{pos}	1.99%
cf_{neg}	-0.521%	μ_{pos}	4.32%	cf_{neg}	-0.278%	μ_{pos}	4.38%
$cf_{y=0}$	5.4%	μ_{neg}	-3.70%	$cf_{y=0}$	4.4%	μ_{neg}	-3.63%
$r_{cf0.8}$	0.52	$x_{y=0}$	53.84%	$r_{cf0.8}$	0.50	$x_{y=0}$	54.70%
P_{min}	-49.44%	$Cor_{RES\text{-}load}$	35.24%	P_{min}	-26.46%	$Cor_{RES\text{-}load}$	46.81%
P_{max}	89.08%			P_{max}	71.69%		

11 The residual load is defined as the total system load minus fluctuating RES generation.

In both scenarios, the very high RES penetration of 47.6% has a strong effect on the remaining residual load duration curve (see Figure 5.3 and Figure 5.4).

The reduction of both the area under the curve and the capacity factor cf_{pos} compared to the load duration curve indicate RES generation. For both scenarios, zero crossing of the residual duration curve is 3.2% for GER and 4.4% for CA. This means that RES generation exceeds the electricity demand in 3.2% and 4.4% of the 8760 simulated hours. In total, the negative residual load (cf_{neg}) for GER 2030 is -0.285% and -0.278% for CA 2030, or 1.95 TWh and 1.55 TWh in absolute values, respectively.[12] During these time periods it is necessary to either export electricity for greater electricity distribution, or store energy, or limit RES power or introduce DSM to maintain the system in balance. The reduction in the maximal power value P_{max} in CA 2030 to 72% and in GER 2030 to 90% shows that RES' contribution to reducing peak residual load is much higher in CA 2030 than in GER 2030 (see Table 5-1). This is due to a closer correlation between photovoltaic as well as solar thermal generation and the CA 2030 load curve. The higher negative peak P_{min} for GER is caused by the high level of installed RES capacity, in total 162% of the peak load (see Chapter 4). For CA 2030 and GER 2030, P_{min} is in the middle of the day when wind and solar output occur simultaneously. Compared to GER, the lower installed RES capacity in CA results in less extreme RES power supply situations. There is a greater influence of solar generation in CA, and wind and solar strongly affect traditional peak load hours particularly during the spring months when high cooling loads are not online (see Figure 5-1).

For a high penetration of fluctuating RES, it will no longer be possible to make a clear distinction between base load during nighttime hours and peak load periods during the day. Figure 5-1 illustrates that peak hours (section 3) during the night that are likely for both scenarios. A peak residual load is most likely during the early evening. For CA 2030, a morning peak is also observed between 6 and 8 a.m. caused by the characteristics of wind generation here. In CA high generation from wind during the morning hours is unlikely. Peak wind output occurs in early evening (see Appendix and [20]). Very high peak hours (section 4) accumulate between 5 and 9 p.m. Noon is characterized by a high frequency of off-peak periods (section 1). Obviously, a lack of solar generation still results in a peak load during the day, but the residual load is likely to be low. From a

[12] Absolute value = relative value * 8760 * $P_{max,\ absolute}$

RES fluctuation point of view, grid integration of RES-E in CA 2030 is less complex because of the higher load, RES-E correlation as well as lower RES capacity with equal energy output (installed capacity is 96.7% of the peak load versus 162% for GER 2030).

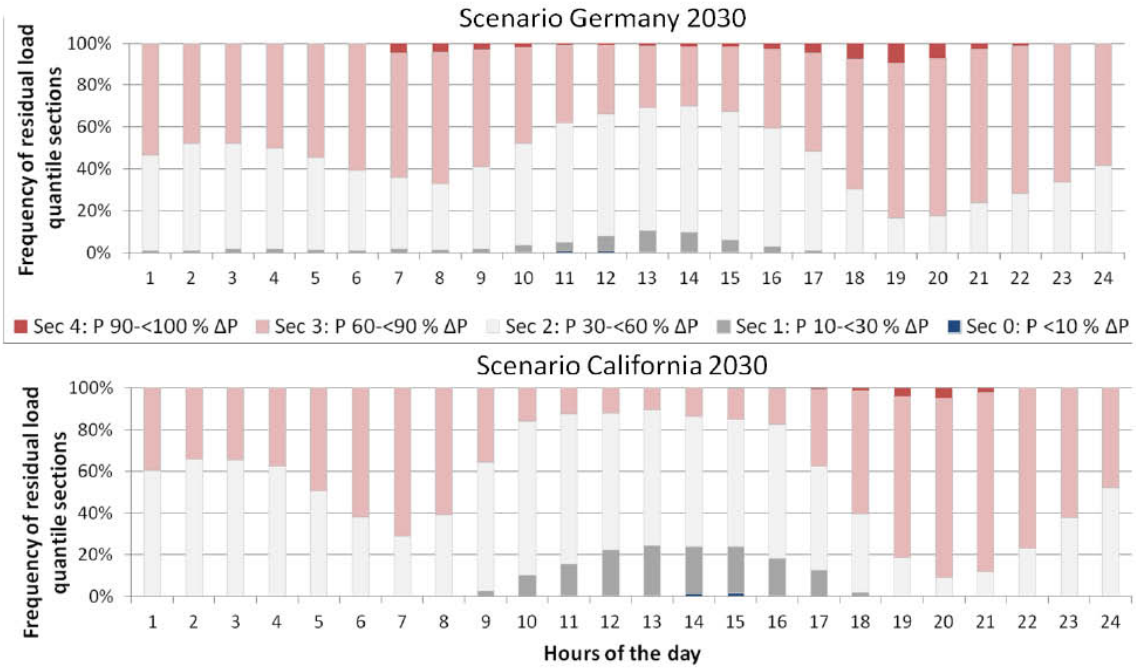

Figure 5-1: Frequency of residual load variation for different hours of the day

CA 2030: $P_{max,load}$ = 63.55 GW, $P_{max,RS}$ =45.55 GW, $P_{min,RS}$ = -16.81 GW, ΔP_{RS}=62.37 GW
GER 2030: $P_{max,load}$ = 77.95 GW, $P_{max,RS}$ =70.44 GW, $P_{min,RS}$ = -33.92, ΔP_{RS}=104.36 GW

For both scenarios, ramping is in the same range with a rrf around 2%. Compared to the system load, for the residual load an increase in total ramping is observed (compare Table 5-1 and 2-6; GER 2030: *rrf* change from 1.19% to 2.03%; CA 2030: *rrf* change from 1.05% to 1.99%). Further, the intensity of the ramp rates μ increase due to the higher penetration of fluctuating RES.

5.1.1 Last trip charging

Charging EVs immediately after returning from the last trip of the day affects the peak load. The simultaneousness of PEV charging is influenced by driving behavior and the grid connection power. The mobility behavior simulation yields a yearly driving distance of 15.3 thousand kilometers per vehicle. The electric driving share is 54%, resulting in an average electricity consumption of 1594 kWh per year. In total, the PEV fleet's demand is 19.2 TWh for GER 2030 and 10.8 TWh for CA 2030.

The peak load increase resulting from uncontrolled charging is determined by the correlation of the initial load curve and PEV charging. For the CA 2030 scenario, this correlation is smaller than for GER 2030. For CA, the hourly mean load increases by about 7.7% whereas, for GER 2030, the increase is 10.2% (compare P_{max} in Table 5-1 and Table 5-2). It should be noted that GER driving data is used here for CA. This could explain the higher correlation of vehicle electricity demand and load curve in GER. For both scenarios there are only minor reductions in the time period with negative residual load ($cf_{x=0}$), the negative peak (P_{min}) and the amount of negative residual load (cf_{neg}). The negative residual load consumed by PEV charging is 11.3% for GER 2030 and 17.1% for CA 2030.

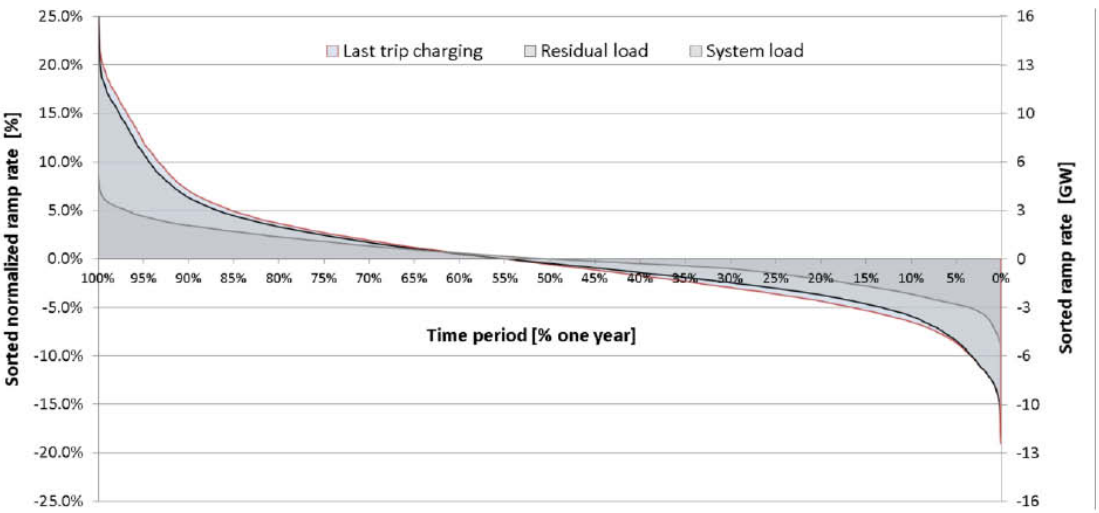

Figure 5-2: Ramp rates for the CA 2030 scenario

The effect of last trip charging on the ramp rates for CA 2030 is shown in Figure 5-2. The ramping increases largely due to the fluctuating generation (see system load versus residual load in Figure. 5-2 and compare Table 5-1 with Table 5-2). The additional increase caused by charging PEVs is small. In conclusion, fluctuating RES-E have a much greater effect on the ramp rates than charging PEVs.

Table 5-2: Evaluation parameter, last trip charging, California (CA) versus Germany (GER).

RS + PEVs last trip charging GER 2030				RS + PEVs last trip charging CA 2030			
cf_{pos}	41.6%	rrf_{pos}	2.32%	cf_{pos}	30.8%	rrf_{pos}	2.20%
cf_{neg}	-0.253%	μ_{pos}	5.06%	cf_{neg}	-0.230%	μ_{pos}	4.87%
$cf_{y=0}$	3.00%	μ_{neg}	-4.25%	$cf_{y=0}$	4.00%	μ_{neg}	-4.00%
$r_{cf0.8}$	0.52	$x_{y=0}$	54.34%	$r_{cf0.8}$	0.52	$x_{y=0}$	54.91%
P_{min}	-42.59%	$Cor_{RES\text{-}load+PEV}$	27.63%	P_{min}	-25.57%	$Cor_{RES\text{-}load+PEV}$	40.20%
P_{max}	100.59%			P_{max}	79.18%		

5.2 Time-of-use tariff

To evaluate the load management with time-of-use tariffs an available tariff of the utility Pacific Gas and Electric [51] is implemented in the simulation as control signal. The tariff structure follows the classical expectations of base and peak load in California and does not account for a high share of RES-E. The tariff is used because it is an example for one of the first tariffs available. Other TOU tariffs would provide similar results, if analyzed with regard to automated control.

Table 5-3: Electric vehicle time-of-use tariff of Pacific Gas and Electric

	Super Off Peak	**Off Peak**	**Peak**	**Off Peak**
Time period	Midnight – 5 am	5 am – 12 pm	12 pm – 6 pm	6 pm - Midnight
Rate	14.4ct/kWh	16.7ct/kWh	25.7ct/kWh	16.7ct/kWh

Source: Data basis [51]

The tariff is divided in four time periods and three price levels (see Table 7-6). The Californian load curve and PEVs penetration as defined in Chapter 6.1 serves as an example. The result of a one week simulation using the TOU tariff indicates two main price peaks (see Figure 5-3). After the first trip in the morning PEVs' agents accomplish to reload the battery in the off peak period 5 am - 12 pm to avoid the peak rate starting at 12 pm. The recharge after the first trip is necessary to realize a high electric driving share. The second peak is observed

before 5 am. This results from the applied optimization algorithm that chooses the last possible time step to charge, if cost of several time steps are equal.[13]

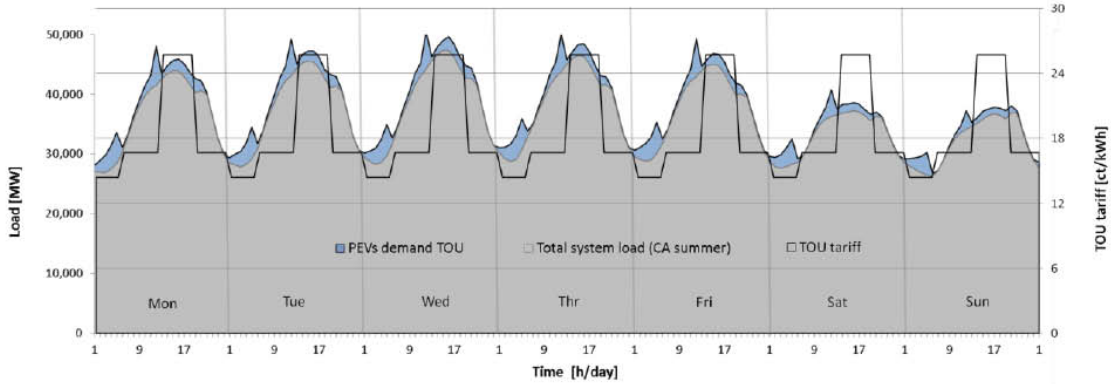

Figure 5-3: Electric vehicle load with time-of-use tariff control

Remarks: Summer week in scenario CA 2030; Source: time-of-use (TOU) tariff [51]; load curve [20]

Analyzing the evaluation parameter (see Table 5-4) shows that TOU rates do not significantly improve the contribution of PEVs as a grid resource compared to last trip charging. For CA 2030, a peak load reduction is observed (P_{max} is reduced from 79% to 74%) and a possible consumption of 39% of negative residual load versus 17% in the case of last trip charging (compare cf_{neg} in Table 5-1, 7-5 and 5-4). With regard to P_{min} and ramping improvements are smaller.[14] For GER 2030, parameter changes compared to last trip charging are in the same range as for CA values. Only the peak reduction is lower because the GER peak load occurs in the evening. The TOU rate used is designed to reduce peak load during the day.

13 In terms of battery aging, using the last possible time step for recharging is not groundless because a high state of charge can account for reduced calendar lifetime.

14 Note: In CA, P_{min} occurs during the day when the TOU rate is high and PEVs therefore avoid charging.

Table 5-4: Evaluation parameters, time-of-use, charging California (CA) versus Germany (GER)

RS + PEVs TOU charging GER 2030				RS + PEVs TOU charging CA 2030			
cf_{pos}	42.4 %	rrf_{pos}	2.35 %	cf_{pos}	31.3 %	rrf_{pos}	2.20 %
cf_{neg}	-0.191 %	μ_{pos}	4.49 %	cf_{neg}	-0.170 %	μ_{pos}	4.37 %
$cf_{y=0}$	2.20 %	μ_{neg}	-4.88 %	$cf_{y=0}$	3.20 %	μ_{neg}	-4.42 %
$r_{cf0.8}$	0.49	$x_{y=0}$	47.87 %	$r_{cf0.8}$	0.47	$x_{y=0}$	49.72 %
P_{min}	-42.15 %	$Cor_{RES\text{-}load+PEV}$	35.36 %	P_{min}	-24.57 %	$Cor_{RES\text{-}load+PEV}$	49.65 %
P_{max}	98.50 %			P_{max}	74.40 %		

The simultaneous reaction of automated agents and the changing requirements in terms of peak and off peak hours due to RES-E (see Figure 5-3) indicate that smart grid control must provide more sophisticated solutions to reduce demand peaks and account for the integration of fluctuating generation.

5.3 Balancing fluctuation with demand-side management

Simulating dynamic pricing with a distributed vehicle-based optimization (see chapter 3) illustrates the contribution of PEVs to balancing fluctuating RES using demand-side management. Evaluation parameters quantifying the effect of DSM smart charging are summarized in Table 5-5.

Compared to last trip charging, the average electricity consumption here increases to 2061 kWh per vehicle with an electric driving share of 70%. This increase is caused by the greater availability of infrastructure. For last trip charging, infrastructure is available after the last trip, which is mainly at home. In the case of DSM, a perfect availability of charging infrastructure is assumed. In total, the PEV fleet consumes 25 TWh (GER 2030) and 14.0 TWh (CA 2030), accounting for approximately 5% of the total electricity demand.

Table 5-5: Evaluation parameters, demand-side management, charging California (CA) versus Germany (GER)

RS + PEVs DSM charging GER 2030				RS + PEVs DSM charging CA 2030			
cf_{pos}	42.3%	rrf_{pos}	1.52%	cf_{pos}	31.2%	rrf_{pos}	1.70%
cf_{neg}	-0.102%	μ_{pos}	2.88%	cf_{neg}	-0.076%	μ_{pos}	3.43%
$cf_{y=0}$	1.40%	μ_{neg}	-3.20%	$cf_{y=0}$	1.60%	μ_{neg}	-3.33%
$r_{cf0.8}$	0.48	$x_{y=0}$	47.35%	$r_{cf0.8}$	0.46	$x_{y=0}$	50.71%
P_{min}	-34.02%	$Cor_{RES\text{-}load+PEV}$	44.50%	P_{min}	-18.52%	$Cor_{RES\text{-}load+PEV}$	56.56%
P_{max}	91.93%			P_{max}	72.09%		

The effect of controlled PEV charging on the residual load duration curve is shown for Germany and California in Figures 5-4 and 5-5, respectively. In both cases, it is possible to limit peak load and increase consumption of the negative residual load. For GER 2030 about 64.0% and for CA 2030 about 72.6% of the negative residual load can be consumed (see Table 5-6 Relative values cf_{neg}). The time period with negative residual load is reduced by 158 hours (GER 2030) and 245 hours (CA 2030). The negative residual peak reduction is 7.4 GW for GER and 5.1 GW for CA (see Table 5-6 Absolute change).

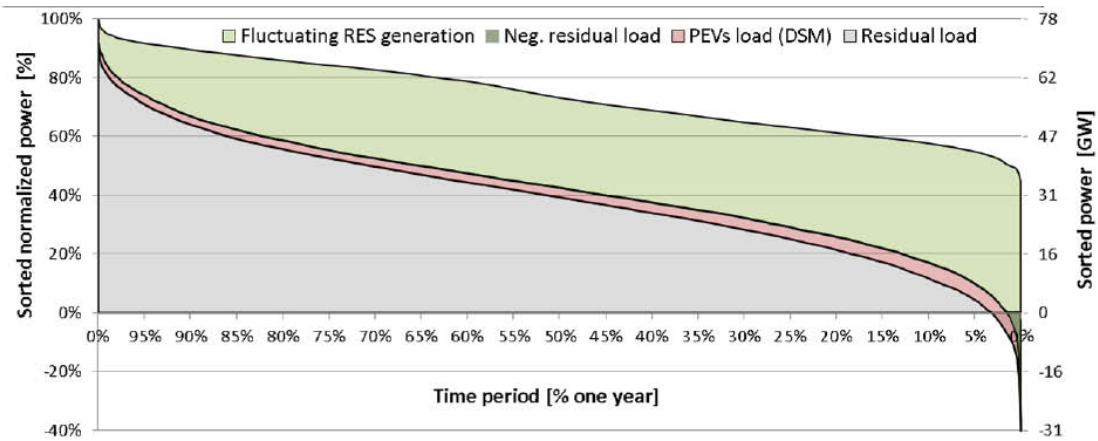

Figure 5-4: Change in the residual load duration curve due to demand-side management for Germany

In terms of ramping, a significant ramp rate factor reduction is achieved of 34.3% for GER and 22.5% for CA. In addition, the ramping mean and the standard deviation values are significantly lower.

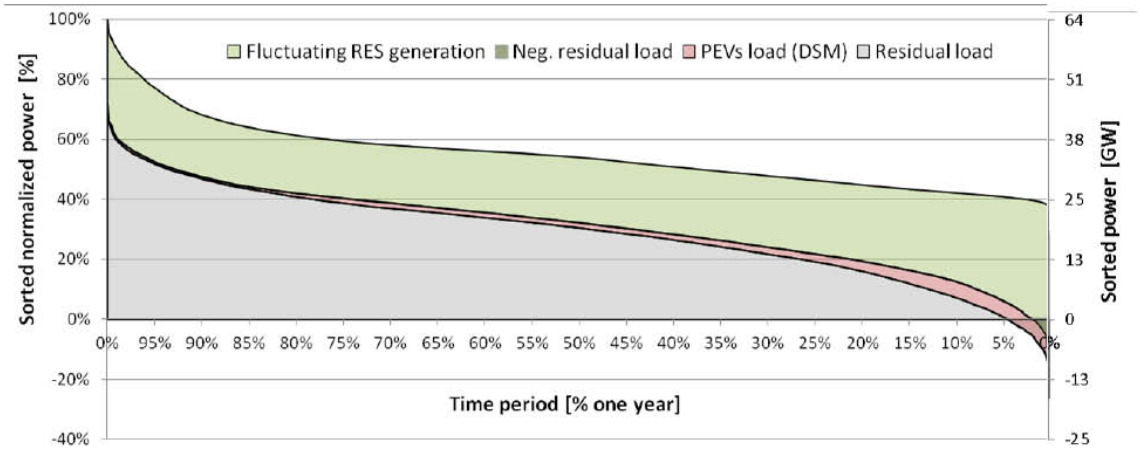

Figure 5-5: Change in the residual load duration curve due to demand-side management for California

PEVs make a greater contribution to integrating RES-E in terms of negative residual load consumption and reducing peak load in CA 2030 than in GER. This indicates that these two parameters are influenced by the RES generation characteristics and the resulting residual load, respectively. For GER 2030, RES generation and partially hours with negative residual load are dominated by wind. The wind generation output for GER is characterized by longer high production periods whereas generation tends to follow a rhythmic daily pattern for CA, especially during the spring and summer (see Appendix and [20]). A daily rhythm is preferable for RES-E grid integration using PEVs, because driving behavior also follows a daily pattern and does not permit long load shifting periods. Refilling the PEV's battery is only possible, if electricity has been consumed for driving. This effect is enhanced by the higher RES capacity required in GER 2030 to produce the same RES electricity output.

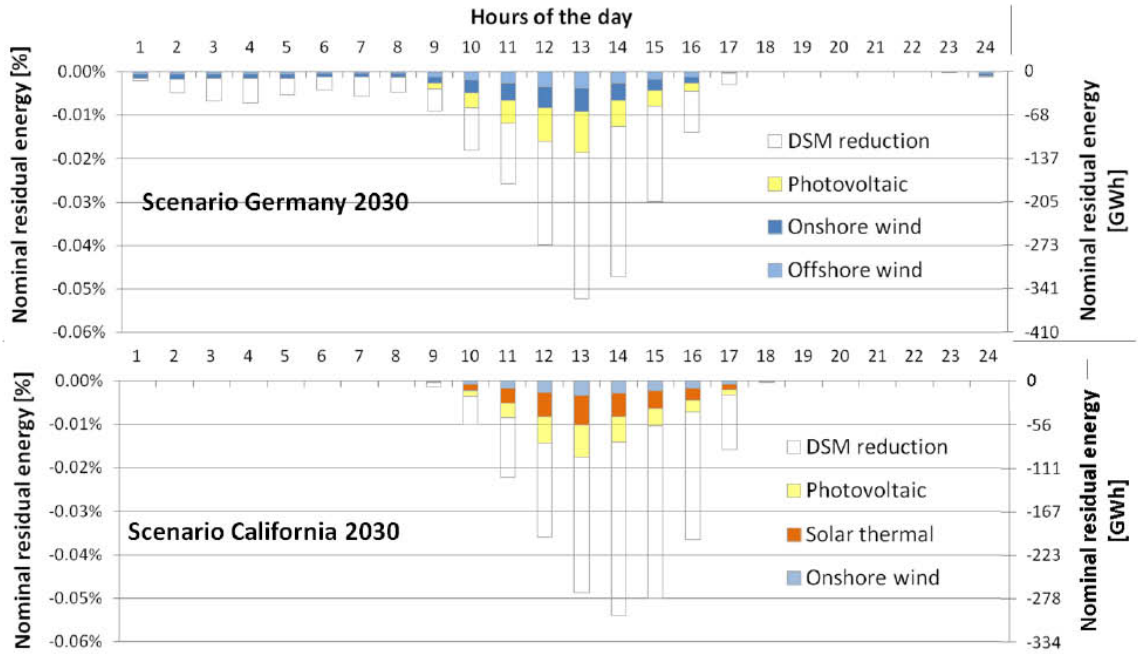

Figure 5-6: Hourly reduction of negative residual energy for California and Germany

Figure 5-6 shows that negative residual energy occurs only during the day for CA 2030. The scenario is dominated by solar generation[15] and RES-E output follows a more daily pattern. Comparing the relative and the absolute change between the residual load without PEVs and the residual load with PEVs for GER 2030 and CA 2030 shows that there is a greater reduction of cf_{neg} and $cf_{y=0}$ for CA 2030 (see Table 5-6). This indicates that solar power is well integratable. The correlation increase is higher for GER 2030 (see values of *Cor* in Tab. 5-6). This also reflects a better integration of solar because the correlation of load and solar generation is lower for GER 2030 than for CA 2030.

15 Solar sources provide about 24% and 11% of total electricity demand for CA 2030 and GER 2030, respectively.

Table 5-6: Change of evaluation parameters, demand-side management charging versus no electric vehicles for California (CA) and Germany (GER)

	Relative values		Absolute values		
Factor	**GER 2030**	**CA 2030**	**GER 2030**	**CA 2030**	**Unit**
cf_{pos}	8.96%	8.04%	23.75	12.92	TWh
cf_{neg}	-64.02%	-72.58%	1.24	1.12	TWh
$cf_{y=0}$	-56.25%	-63.64%	-158	-245	hour
P_{min}	-21.83%	-30.02%	7.41	5.05	GW
P_{max}	1.73%	0.56%	1.22	0.26	GW
rrf_{pos}	-34.27%	-22.51%	-4.76	-2.49	TWh
μ_{pos}	-43.10%	-29.65%	-1.48	-0.83	GW
μ_{neg}	-24.73%	-16.74%	0.72	0.39	GW
Cor	30.03%	20.81%	10.28%	9.74%	%

6 Conclusions

This paper investigated how grid-connected electric vehicles can contribute to integrating fluctuating renewable generation sources. The study used an agent-based simulation model including real-time prices as control signals and a detailed simulation of driving behavior.

Country-specific time series and installed capacities for solar and wind power were considered for the two case studies of Germany and California. The comparison of these two countries shows that the resulting residual load is strongly affected by the assumptions concerning the installed capacity of renewable energy sources and by the time series used. Therefore, studies of integrating fluctuating generation should include a detailed description of the time series used and the resulting residual load scenarios. The findings for Germany (GER) and California (CA) under the scenario assumptions made for 2030 with high shares of RES-E and PEVs are:

- The capacity factors of wind and photovoltaics are lower in GER than in CA. Hence, a higher installed capacity is needed to generate the same amount of energy in Germany. For both countries, the energy produced from fluctuating RES represents 47% of the total system load. The installed RES capacity as percentage of the system peak load is 162% and 97% for GER and CA, respectively. The higher installed capacity results in more extreme RES surplus generation or negative residual load situations in the GER scenario.

- The ramping of the residual load is strongly influenced by RES generation. Compared to the load curve without considering RES generation, ramping nearly doubles if fluctuating generation is included. This is the case for both CA and GER. In terms of single time series, especially PV in CA has very high ramp rates. Possible reasons are the higher direct radiation in CA and the resulting system specifications (trekking systems, solar thermal power using storage, and concentration of installations to a specific region). In addition, the method of calculating the time series can influence the results. For GER, offshore wind shows higher ramp rates compared to onshore wind.
- Besides the energy produced by a renewable energy technology, its fluctuation characteristic also plays an important role when evaluating the contribution of storage technologies to grid integration. In terms of photovoltaics, the characteristics on sunny days are obviously very similar in both GER and CA. Taking the entire year into account, however, reveals an on/off characteristic for GER. Or, in other words, days with almost no generation occur more often in GER, particularly during the winter, but also during the summer, albeit with reduced probability. Solar generation is much more reliable in CA and even for wind, generation here is characterized by a regular daily pattern for large periods of the year. In GER, there is a greater dependence on specific weather fronts for wind generation. To sum up, periods lasting several days with very high wind velocities and periods with almost no wind are more likely in GER than in CA.
- In this context, besides the characteristics of the individual generation technology, it is also very important to account for the overall outcome of the technology mix and the resulting residual load. The correlation between load and the expected output of total RES generation strongly affects the situation in a power system. A higher correlation is found between the expected RES generation scenarios and load for CA than for GER. This is due to the daily pattern of generation in CA being a match for the load curve, which also follows a daily pattern. In addition, the air conditioning load and solar generation which dominate Californian summers, evidently account for a high level of correlation.
- The residual load in both simulation scenarios indicates a drastic change taking place in the power system, if renewable energies become a dominant generation source. In this case, peak hours at noon and during the early afternoon are unlikely. This time of the day is dominated by a low residual load. A high peak hour probability is observed during early evening and nighttime hours. For CA, the morning hours are also expected to account for high residual loads. This does not mean that typical peak load events which follow the load curve are no longer possible. However, they are less likely and it will no longer be possible to describe the residual load for the entire year based on a few characteristic days.

To investigate the effect of grid-connected vehicles on the power system, three charging strategies were distinguished: charging after the last trip, TOU charging and demand-side management (DSM). In terms of last trip charging, the results presented here are in accordance with other publications. Additional findings are:

- Last trip charging results in a reduced electric driving share of 54% compared to 70% with DSM assuming that infrastructure is available at home and at work. This finding strongly depends on the assumed driving behavior and battery size of the modeled vehicles.
- Last trip charging increases the ramp rates in the power system. With the used time increment of one hour, however, the increase is low compared to the effect of fluctuating generation. The increase in the ramp rate factor is 10 to 15%.
- Overall, PEVs only make a small contribution to balancing RES-E and only a small proportion of surplus energy from RES or negative residual load can be consumed in the case of last trip charging.

TOU charging can be a first approach for peak load reduction and off-peak charging. In case of regular residual load pattern TOU rates also can contribute to integrate fluctuating RES-E. For a strong event-based RES generation TOU rates are too inertial and cannot provide an effective integration of fluctuating RES-E.

There have also been previous studies made that analyze DSM using grid-connected vehicle loads (e.g. [52]; [16]). In addition to these publications, the PowerACE DSM model includes a detailed simulation of individual driving behavior and a control mechanism based on real-time pricing and distributed optimization from the perspective of vehicles acting as independent agents. Furthermore, power systems with a high share of fluctuating RES generation were assumed. The results in detail are:

- DSM is restricted by mobility behavior. If consumers maximize the electric range of their vehicles to recoup their initial investment, the peak load increases even with load management.
- DSM can strongly reduce ramp rates and surplus energy consumption from RES-E. Detailed evaluation parameters, which are discussed in the results section, quantify this effect.
- Comparing CA and GER reveals that more effective use can be made of electric vehicles as a grid resource in CA due to the characteristics of RES-E and the resulting residual load here. This is because grid-connected vehicle load shifting is only possible within a time period of several hours to one or

two days. The daily pattern of RES power generation in CA makes it easier to integrate.

- The same argument applies, if photovoltaics and wind power are compared with each other. The daily pattern of photovoltaic generation favors the storage capabilities of electric vehicles, if charging infrastructure is available where the vehicles are parked during the day.

This paper highlights the importance of carefully considering load and renewable energy generation output when analyzing future power systems. To better understand research results, a detailed evolution of RES-E time series, system load and residual load is recommended. This paper describes a possible method and the characterization parameters needed to do so.

7 Appendix

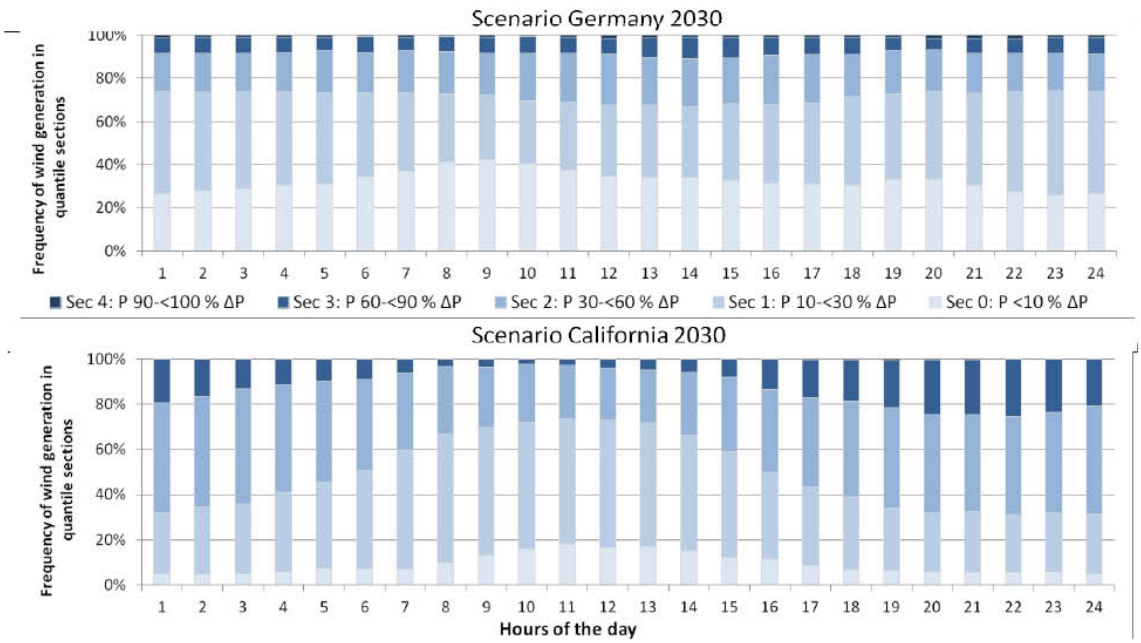

Figure 7-1: Availability of onshore wind generation for different hours of the day

CA 2030: $P_{max,load}$ = 28.23 GW, P_{max} =22.79 GW, P_{min} = 0.57 GW, ΔP= 22.22 GW

GER 2030: $P_{installed}$ = 37.8 GW, P_{max} = 31.19 GW, P_{min} = 0.21, ΔP= 30.98 GW

Table 7-1: Interval availability parameters

	Sec 0						Sec 1					
Time series	$y_{O-0.1}$	$y_{O-0.3}$	**Counts**	t_{mean}	t_{σ}	t_{max}	$y_{O-0.3}$	$y_{O-0.6}$	**Counts**	t_{mean}	t_{σ}	t_{max}
Wind onshore GER	0.6%	8.8%	173	20.5	16.5	134	8.8%	25.1%	173	34.1	61.0	620
Wind offshore GER	0.1%	8.7%	103	7.7	8.4	35	8.7%	25.9%	103	77.2	138.8	982
Photovoltaic GER	0.0%	6.3%	347	16.3	10.1	166	6.3%	18.9%	342	8.6	3.2	13
RES GER 2008	0.5%	11.3%	167	7.5	5.6	38	11.3%	32.9%	167	44.9	83.2	622
Load GER 2008	44.7%	50.2%	30	3.9	2.0	8	50.2%	61.3%	30	286.0	653.9	2900
RS GER 2008	-43.5%	-30.1%	2	4.0	2.8	6	-30.1%	-3.4%	50	4.0	2.3	10
Wind onshore CA	2.0%	9.9%	122	6.6	7.2	42	9.9%	25.6%	122	64.9	127.8	794
Solar thermal CA	0.0%	9.6%	229	15.2	5.2	44	9.6%	28.7%	266	9.8	2.4	12
Photovoltaic CA	0.0%	9.8%	365	13.3	1.5	17	9.8%	29.5%	325	10.7	1.6	13
RES CA	1.2%	8.4%	170	6.4	5.0	17	8.4%	22.7%	170	45.0	106.2	886
Load CA	36.3%	42.7%	240	4.5	2.0	11	42.7%	55.4%	240	31.9	118.1	1822
RS CA	-26.5%	-16.6%	5	2.6	1.9	6	-16.6%	3.0%	5	3.6	1.5	6

	Sec 2						Sec 3					
Time series	$y_{O-0.3}$	$y_{O-0.6}$	**Counts**	t_{mean}	t_{σ}	t_{max}	$y_{O-0.6}$	$y_{O-0.9}$	**Counts**	t_{mean}	t_{σ}	t_{max}
Wind onshore GER	25.1%	49.7%	100	24.8	29.3	131	49.7%	74.3%	47	15.9	14.0	58
Wind offshore GER	25.9%	51.6%	214	27.1	50.6	511	51.6%	77.3%	195	16.0	19.5	88
Photovoltaic GER	18.9%	37.9%	266	7.3	2.7	11	37.9%	56.8%	149	5.0	2.0	8
RES GER 2008	32.9%	65.4%	271	16.0	21.4	144	65.4%	97.8%	134	6.0	4.8	33
Load GER 2008	61.3%	77.9%	283	24.6	35.0	162	77.9%	94.5%	280	13.1	4.7	19
RS GER 2008	-3.4%	36.8%	50	166.7	185.4	718	36.8%	77.0%	338	14.1	22.2	140
Wind onshore CA	25.6%	49.3%	267	16.7	19.3	132	49.3%	72.9%	168	6.7	6.1	41
Solar thermal CA	28.7%	57.4%	131	7.1	2.8	11	57.4%	86.1%	194	6.3	2.2	9
Photovoltaic CA	29.5%	59.1%	360	8.7	1.9	11	59.1%	88.6%	304	6.0	1.5	8
RES CA	22.7%	44.2%	370	10.9	9.5	117	44.2%	72.9%	271	6.5	2.3	11
Load CA	55.4%	74.5%	412	9.2	5.7	20	74.5%	93.6%	66	8.2	3.7	13
RS CA	3.0%	32.4%	105	76.8	203.2	1651	32.4%	61.9%	480	8.1	9.8	117

	Sec 4					
Time series	$y_{O-0.9}$	y_{O-1}	**Counts**	t_{mean}	t_{σ}	t_{max}
Wind onshore GER	74.3%	86%	16	6.1	3.8	17
Wind offshore GER	77.3%	83%	131	4.5	4.7	26
Photovoltaic GER	56.8%	63%	24	2.8	0.9	4
RES GER 2008	97.8%	109%	7	3.0	1.2	4
Load GER 2008	94.5%	100%	60	2.0	1.1	5
RS GER 2008	77.0%	90%	62	3.1	2.6	14
Wind onshore CA	72.9%	81%	2	3.0	0.0	3
Solar thermal CA	86.1%	96%	175	4.6	2.6	8
Photovoltaic CA	88.6%	98%	80	2.2	1.0	4
RES CA	72.9%	73%	21	3.2	1.8	6
Load CA	93.6%	100%	13	2.8	1.2	5
RS CA	61.9%	71.7%	19	2.5	1.0	4

Note: CA: California base year of time series 2005; GER: Germany reference year of time series 2008; Source: Own calculation data basis [20], [24], [28].

8 Acknowledgements

This work has been co- financed under grant of the German Federal Ministry for the Environment, Nature Conservation and Nuclear Safety (BMU) and E.ON AG as part of the project "Flottenversuch Elektromobilität". We thank Patrick Plötz, Peter Cappers, Andrew Mills, Thomas Schnepf and Gillian Bowman-Köhler for discussions, providing information on renewable energy sources and critical reading of the manuscript.

9 References

[1] Awerbuch, S. (2006) Portfolio-Based Electricity Generation Planning: Policy Implications For Renewables And Energy Security, Mitigation and Adaptation Strategies for Global Change Volume 11, Number 3, 693-710, DOI: 10.1007/s11027-006-4754-4

[2] Gustav Resch, Anne Held, Thomas Fabera, Christian Panzera, Felipe Toro, Reinhard Haasa (2008) Potentials and prospects for renewable energies at global scale, Energy Policy Volume 36, Issue 11, Pages 4048–4056.

[3] Tomić, J., Kempton, W. (2007). Using fleets of electric-drive vehicles for grid support. Journal of Power Sources 168, 459-468

[4] Stadler, I. (2006) Power grid balancing of energy systems with high renewable energy penetration by demand response, Utilities Policy 16 (2008) 90e98

[5] J. Link, M. Büttner, D. Dallinger, J. Richter, Optimisation Algorithms for the Charge Dispatch of Plug-in Vehicles based on Variable Tariffs, Working Paper Sustainability and Innovation, 2010. Retrieved: 11. July 2011, URL: http://econstor.eu/bitstream/10419/36697/1/623961075.pdf

[6] Cappers, P., Mills, A., Goldman, C., Wiser, R., Eto, J. H. (2011). Mass Market Demand Response and Variable Generation Integration Issues: A Scoping Study, Environmental Energy Technologies Division, Lawrence Berkeley National Laboratory, Prepared for the Office of Electricity Delivery and Energy Reliability U.S. Department of Energy, LBNL-5063E

[7] Barbose, G., Goldman, C., Bharvirkar, R., Hopper, N., Ting, M. and Neenan, B. (2005). Real Time Pricing as a Default or Optional Service for C&I Customers: A Comparative Analysis of Eight Case Studies. Lawrence Berkeley National Laboratory, Berkeley, CA. Prepared for California Energy Commission. LBNL-57661.

[8] F. A. Wolak, An Experimental Comparison of Critical Peak and Hourly Pricing: The Power Cents DC Program, Department of Economics Stanford University, 2010. Retrieved: 11. July 2011, URL: http://sedc-coalition.eu/wp-content/uploads/2011/06/Wolak-10-03-15-PowerCentsDC-Paper.pdf

[9] M. Pehnt, H. Helms, U. Lambrecht, D. Dallinger, M. Wietschel, H. Heinrichs, R. Kohrs, J. Link, S. Trommer, T. Pollok, P. Behrens, Elektroautos in einer von erneuerbaren Energien geprägten Energiewirtschaft, Zeitschrift für Energiewirtschaft, 2011.

[10] P. Denholm, W. Short, An Evaluation of Utility System Impacts and Benefits of Optimally Dispatched Plug-In Hybrid Electric Vehicles An Evaluation of Utility System Impacts and Benefits of Optimally Dispatched Plug-In Hybrid Electric Vehicles, Technical Report NREL/TP-620-40293, 2006. Retrieved: 11. July 2011, URL: www.nrel.gov/docs/fy07osti/40293.pdf

[11] Green II RC,Wang L, Alam M. The impact of plug-in hybrid electric vehicles on distribution networks: a review and outlook. Renewable and Sustainable Energy Reviews 2011;15:544e53

[12] R. McCarthy, C. Yang, C., Determining marginal electricity for near-term plug-in and fuel cell vehicle demands in California: impacts on vehicle greenhouse gas emissions, Journal of Power Sources 195, April 2010, pp. 2099–2109.

[13] Dallinger, D., Wietschel, M., Santini D. J. (2012). Effect of demand response on the marginal electricity used by plug-in electric vehicles, 26th Electric Vehicle Symposium, May 6-9, 2012 in Los Angeles, California

[14] H. Lund, W. Kempton, Integration of renewable energy into the transport and electricity sectors through V2G, Energy Policy, vol. 36, 2008, pp. 3578-3587.

[15] Markel, T., Kuss, M., Denholm, P. (2009). Communication and control of electric drive vehicles supporting renewable, Vehicle Power and Propulsion Conference, 2009. VPPC '09. IEEE

[16] J. Wang, C. Liu, D. Ton, Y. Zhou, J. Kim, A. Vyas, Impact of plug-in hybrid electric vehicles on power systems with demand response and wind power, Energy Policy, vol. 39, 2011, pp. 4016-4021.

[17] Sørensen, P, and NA Cutululis. 2007. “Power fluctuations from large wind farms.” IEEE Transactions on Power Systems, 22 (3): 958-965. http://ieeexplore.ieee.org/xpls/abs_all.jsp?arnumber=4282056.

[18] M.B. Blarke, H. Lund, The effectiveness of storage and relocation options in renewable energy systems, Renewable Energy 33 (2008) 1499–1507

[19] Holttinen, H. (2005). Hourly Wind Power Variations in the Nordic Countries. Wind Energy Volume 8, Number 2 , P. 173-195.

[20] CAISO, (2011), 33 percent trajectory case - preliminary new scenarios: File “One-Minute Data for Load, Wind and Solar” (3/14/2011 07:44) and “Step 1 Assumptions, Forecast Errors and Renewable Profiles” (3/11/2011 15:23), California Independent System Operator, Retrieved: 24. October 2011, URL: http://www.caiso.com/Documents/33%20percent%20trajectory%20case%20-%20preliminary%20new%20scenarios

[21] Solar Anywhere. 2011. “Satellite solar irradiance data.” Accessed July 11, 2011. https://www.solaranywhere.com/Public/About.aspx.

[22] CPUC: California Public Utilities Commission. 2012. “Renewable Integration Workshops.” Accessed March 31, 2012. http://www.cpuc.ca.gov/PUC/energy/Renewables/100824_workshop.htm.

[23] NREL (2009), “Western Wind Resources Dataset,” National Renewable Energy Laboratory, Retrieved: 11. July 2011, URL: http://www.nrel.gov/wind/westernwind

[24] EEX (2011). Transparency in Energy Markets - Gesetzliche Veröffentlichungspflichten der Übertragungsnetzbetreiber. European Energy Exchange AG -Transparenzplattform. Retrieved: 11. July 2011, URL: http://www.transparency.eex.com/de/.

[25] Meteomedia AG (2009). Meteorologischer Datensatz. Gais, Schweiz.

[26] SoDa Web Service. 2011. Solar irradiation data from HC3hourDNI.

[27] Schubert, Gerda. (2010) “Modellierung der Stromeinspeisung aus Windenergie für ein europäisches Strom, Fraunhofer ISI and University of Flensburg.

[28] Schubert, Gerda. (2011) “Modellierung der stündlichen regionalen Photovoltaik- und Windstromeinspeisung in Europa auf Basis meteorologischer Daten.” Fraunhofer ISI and University of Flensburg.

[29] Sørensen, P, and NA Cutululis. 2007. “Power fluctuations from large wind farms.” IEEE Transactions on Power Systems, 22 (3): 958-965. http://ieeexplore.ieee.org/xpls/abs_all.jsp?arnumber=4282056.]

[30] Gottschall, Julia, and Joachim Peinke. 2007. “Stochastic modelling of a wind turbine’s power output with special respect to turbulent dynamics.” Journal of Physics: Conference Series 75 (July 1): 012045. doi:10.1088/1742-6596/75/1/012045. http://stacks.iop.org/1742-6596/75/i=1/a=012045?key=crossref.89105324e92c1ae7bef48bb5ab7718c5.

[31] Ensslin, Cornel, Michael Milligan, Hannele Holttinen, Mark O’Malley, and Andrew Keane (2008) “Current methods to calculate capacity credit of wind power, IEA collaboration.” 2008 IEEE Power and Energy Society General Meeting - Conversion and Delivery of Electrical Energy in the 21st Century (July): 1-3. doi:10.1109/PES.2008.4596006. Retrieved: 11. July 2011, URL: http://ieeexplore.ieee.org/lpdocs/epic03/wrapper.htm?arnumber=4596006

[32] SWK: Stadtwerke Karlsruhe GmbH. 2010. “Time series of wind and solar generation.” Obtained from Dr. Ing. Thomas Schnepf, Stabsstelle Strategische Planung, October 28, 2010

[33] McLean, J. R. (2008) Trade Wind WP 2.6 – Equivalent Wind Power Curves. Power, Retrieved: 11. July 2011, URL: http://www.trade-wind.eu/fileadmin/documents/publications/D2.4_Equivalent_Wind_Power_Curves_11914bt02c.pdf.

[34] Sensfuß, F. (2007). Assessment of the impact of renewable electricity generation on the German electricity sector - An agent-based simulation approach, University of Karlsruhe (TH), 2007

[35] Sensfus, F, M Ragwitz, and M Genoese. 2008. “The merit-order effect: A detailed analysis of the price effect of renewable electricity generation on spot market prices in Germany.” Energy Policy 36 (8) (August): 3086-3094. doi:10.1016/j.enpol.2008.03.035. http://linkinghub.elsevier.com/retrieve/pii/S0301421508001717.

[36] Genoese, F., Genoese, M. & Wietschel, M., (2010). In Occurrence of negative prices on the German spot market for electricity and their influence on balancing power markets. EEM2010 - 7TH INTERNATIONAL CONFERENCE ON THE EUROPEAN ENERGY MARKET

[37] Nicolosi, M., and M. Fürsch. 2009. “The Impact of an increasing share of RES-E on the Conventional Power Market – The Example of Germany.” ZfE Zeitschrift für Energiewirtschaft 03 | 2009. http://www.ewi.unikoeln.de/fileadmin/user_upload/Publikationen/Zeitschriften/2009/09_03_01_Nicolosi_Fuersch_Zfe.pdf.

[38] D. Dallinger, M. Wietschel, Grid integration of intermittent renewable energy sources using price-responsive plug-in electric vehicles, Fraunhofer Institute for Systems and Innovation Research Karlsruhe, Working Paper Sustainability and Innovation No. S 7, 2011.

[39] Nitsch, J., Pregger, T., Scholz, Y., Naegler, T., Sterner, M., Gerhardt, N., Von Oehsen, A., B Pape, C., Saint-Drean, Y., Wenzel, and . 2010. “Langfristszenarien und Strategien für den Ausbau der erneuerbaren Energien in Deutschland bei Berücksichtigung der Entwicklung in Europa und global.” Deutsches Zentrum für Luft- und Raumfahrt, Fraunhofer Institut für Windenergie und Energiesystemtechnik, Ingenieurbüro für neue Energien BMU - FKZ0. Retrieved: 11. July 2011, URL: http://www.erneuerbareenergien.de/files/pdfs/allgemein/application/pdf/leitszenario2009_kurzfassung_bf.pdf.

[40] dena-Netzstudie II: Kohler, S., Agricola, A.-C. & Seidl, H., 2010. Integration erneuerbarer Energien in die deutsche Stromversorgung im Zeitraum 2015 – 2020 mit Ausblick 2025. Deutsche Energie-Agentur GmbH. Retrieved: 11. July 2011, URL: dena-Netzstudie II: http://www.dena.de/fileadmin/user_upload/Download/Dokumente/Studien___Umfragen/Endbericht_dena-Netzstudie_II.PDF

[41] Energieszenarien 2011: Schlesinger, M. et al., (2011) Projekt Nr. 12/10 des Bundesministeriums für Wirtschaft und Technologie. Retrieved: 11. July 2011, URL: http://www.prognos.com/fileadmin/pdf/publikationsdatenbank/11_08_12_Energieszenarien_2011.pdf.

[42] Schulz, W., M. Bartels, C. Gatzen, D. Lindenberger, and F. Müsgens. 2005. "Energiereport IV–Die Entwicklung der Energiemärkte bis zum Jahr 2030, Energiewirtschaftliche Referenzprognose." Köln, Basel: EWI/Prognose.. Retrieved: 11. July 2011, URL: http://www.prognos.com/fileadmin/pdf/Energiereport%20IV_Kurzfassung_d.pdf

[43] METI, (2006). Strategic Technology Roadmap (Energy Sector) - Energy Technology Vision 2100. Ministry of Economy, Trade and Industry. Available at: http://www.iae.or.jp/2100/main.pdf.

[44] Moawad, Ayman, Gurhari Singh, Simeon Hagspiel, Mohamed Fellah, and Aymeric Rousseau. 2009. "Impact of Real World Drive Cycles on PHEV Fuel Efficiency and Cost for Different Powertrain and Battery Characteristics." conference paper EVS24. http://www.transportation.anl.gov/pdfs/HV/564.pdf.

[45] J. Gonder, A. Simpson, Measuring and Reporting Fuel Economy of Plug-In Hybrid Electric Vehicles. The World Electric Vehicle Association Journal, Vol. 1, 2007.

[46] D. J. Santini, A. D. Vyas, J. L. Anderson, Fuel Economy Improvement via Hybridization vs. Vehicle Performance Level. FuelFuture Car Congress 2002 (paper 02FCC-125, Arlington). http://cta.ornl.gov/TRBenergy/trb_documents/santini_fuel_economy.pdf, 2002.

[47] Hadley, Stanton W., and Alexandra a. Tsvetkova. 2009. "Potential Impacts of Plug-in Hybrid Electric Vehicles on Regional Power Generation." The Electricity Journal 22 (10) (December): 56-68. doi:10.1016/j.tej.2009.10.011. http://linkinghub.elsevier.com/retrieve/pii/S104061900900267X

[48] R.W. McCarthy, C. Yang, J.M. Ogden, California Energy Demand Scenario Projections to 2050, UCD-ITS-RR-08-11, Institute of Transportation Studies, University of California, Davis, 2006.

[49] Becker, Thomas A. 2009. “Electric Vehicles in the United States A New Model with Forecasts to 2030.” Center for Entrepreneurship & Technology at the University of California, Berkeley.

[50] California Department of Transportation. 2005. “CALIFORNIA MOTOR VEHICLE STOCK , TRAVEL AND FUEL FORECAST.” Transportation CALIFORNIA. http://www.dot.ca.gov/hq/tsip/smb/documents/mvstaff/mvstaff05.pdf.

[51] Pacific Gas and Electric. 2011. “Electric vehicle time of the use tariff”. Accessed July 11, 2011. http://sdge.com/clean-energy/electric-vehicles/electric-vehicles.

[52] Sioshansi, R, and J Miller. 2011. Plug-in hybrid electric vehicles can be clean and economical in dirty power systems. Energy Policy 39 (10): 6151-6161.

Authors' affiliations

David Dallinger, Gerda Schubert and Martin Wietschel

Fraunhofer Institute for Systems and Innovation Research (Fraunhofer ISI)

Contact: Brigitte Kallfass

Fraunhofer Institute for Systems
and Innovation Research (Fraunhofer ISI)
Competence Center Energy Policy and Energy Markets
Breslauer Strasse 48
76139 Karlsruhe
Germany
Phone: +49 / 721 / 6809-150
Fax: +49 / 721 / 6809-203
E-mail: brigitte.kallfass@isi.fraunhofer.de
URL: www.isi.fraunhofer.de

Karlsruhe 2012